HHS Public Access

Author manuscript

Addict Biol. Author manuscript; available in PMC 2018 May 01.

Published in final edited form as:

Addict Biol. 2017 May ; 22(3): 712–723. doi:10.1111/adb.12364.

Adult Rat Cortical Thickness Changes Across Age and Following Adolescent Intermittent Ethanol Treatment

Ryan P. Vetreno[1], **Richard Yaxley**[1], **Beatriz Paniagua**[1], **G. Allan Johnson**[2], and **Fulton T. Crews**[1]

[1]Bowles Center for Alcohol Studies, Department of Psychiatry, University of North Carolina at Chapel Hill, Chapel Hill, NC 27599 USA

[2]Duke Center for In Vivo Microscopy, Box 3302, Duke University Medical Center, Durham, NC 27710 USA

Abstract

Human studies have established that adolescence is a period of brain maturation that parallels the development of adult behaviors. However, little is known regarding cortical development in the adult rat brain. We used magnetic resonance imaging (MRI) and histology to assess the impact of age on adult Wistar rat cortical thickness on postnatal day (P)80 and P220 as well as the effect of adolescent binge ethanol exposure on adult (P80) cortical thickness. Magnetic resonance imaging revealed changes in cortical thickness between P80 and P220 that differ across cortical region. The adult P220 rat prefrontal cortex increased in thickness whereas cortical thinning occurred in both the cingulate and parietal cortices relative to young adult P80 rats. Histological analysis confirmed the age-related cortical thinning. In the second series of experiments, an animal model of adolescent intermittent ethanol (AIE; 5.0 g/kg, i.g., 20% ethanol w/v, 2-days on/2-days off from P25 to P55) was used to assess the effects of alcohol on cortical thickness in young adult (P80) rats. Magnetic resonance imaging revealed that AIE resulted in region-specific cortical changes. A small region within the prefrontal cortex was significantly thinner whereas medial cortical regions were significantly thicker in young adult (P80) AIE-treated rats. The observed increase in cortical thickness was confirmed by histology. Thus, the rat cerebral cortex continues to undergo cortical thickness changes into adulthood and adolescent alcohol exposure alters the young adult cortex that could contribute to brain dysfunction in adulthood.

Keywords

cortical thickness; adolescence; alcohol; development; binge drinking

Corresponding author: Ryan P. Vetreno, Ph.D., University of North Carolina at Chapel Hill, School of Medicine, Bowles Center for Alcohol Studies, CB #7178, 1021 Thurston-Bowles Building, Chapel Hill, NC 27599-7178, Tel: 1-919-966-0501, Fax: 1-919-966-5679, rvetreno@email.unc.edu.

Author Contributions

RPV, FTC, and GAJ were responsible for the study concept and design. All authors contributed equally to the data preparation and analyses. RPV drafted the manuscript. All authors were involved in manuscript editing and have approved the final version for publication.

Introduction

Adolescence is a conserved neurodevelopmental period in humans characterized by significant brain changes that include cortical expansion and thinning that parallels the transition of the immature brain to the more efficient adult brain (Giedd, 2004; Sowell et al., 2004a; Spear, 2009). Magnetic resonance imaging (MRI) studies in human adolescents reveal an inverted U-shape curve in both cortical gray matter volume and cortical thickness that is characterized by an initial expansion followed by cortical thinning (Brown et al., 2012; Giedd, 2004; Giedd et al., 1999). Adolescent cortical thinning occurs in a caudal to rostral trajectory (Gogtay et al., 2004) with the visual cortex first attaining peak thickness at approximately the 4th month after birth followed by cortical thinning that continues until the preschool years (Toga et al., 2006). As cortical maturation progresses, both the dorsal parietal and primary somatosensory regions undergo cortical thinning at approximately 4 to 8 years of age while maturation of the language and spatial orientation regions of the parietal cortex occur at approximately 11 to 13 years of age, and the prefrontal cortex during late adolescence (Gogtay et al., 2004; Toga et al., 2006). The cortical expansion and retraction that exemplifies the maturing adolescent brain appears to be related to the development of intelligence (Schnack et al., 2014; Shaw et al., 2006). Of import, the trajectory of cortical thickness changes, rather than absolute cortical thickness itself, appears to be most closely related to the development of intelligence (Schnack et al., 2014). Indeed, Shaw and colleagues (2006) found that in children possessing higher IQ levels, the cerebral cortex achieved peak expansion later in adolescence than their peers. While cortical maturation in the adolescent brain has received considerable attention, little is known about cortical thickness changes that occur during adulthood. Studies of gray matter density changes from childhood to old age find changes across the lifespan, with some regions decreasing into adulthood and then stabilizing whereas others remain stable until upper middle and old age (Sowell et al., 2004b). Schnack and colleagues (2014) suggest that cortical development is never complete, but rather shows continued intelligence-dependent development. The increase in cortical plasticity that characterizes the adolescent brain also increases its sensitivity to environmental factors such as alcohol, which is commonly consumed and abused during adolescence.

Adolescent cortical maturation coincides with increased experimentation with alcohol and other drugs of abuse in humans (Windle et al., 2008). Binge drinking, defined as the consumption of 5 or more consecutive alcoholic beverages in a two-hour period, is common during adolescence as 5% of 8th grade, 14% of 10th grade, and 22% of 12th grade individuals reported engaging in binge drinking over the past two weeks (Johnston et al., 2013). This heavy drinking pattern continues through college as 41% of male students report binge drinking every two weeks while 8% of college students report consuming ≥3 times the binge drinking threshold in a single episode during a two-week period (White et al., 2006). Adolescent binge drinking could lead to long-term changes in cerebral cortex development due to the heightened neural plasticity and structural development that characterizes the adolescent brain (Crews et al., 2007). In support, an earlier age of drinking onset (i.e., 11 – 14 years of age) is associated with an increased risk of developing an alcohol use disorder later in life (DeWit et al., 2000). Further, in human adolescent males, binge drinking is

associated with reduced cortical thickness in both the prefrontal and cingulate cortices of male human adolescents (Squeglia et al., 2012) as well as diminished impulse inhibition and impaired executive functioning (White et al., 2011), which is consistent with the hypothesis that adolescent binge drinking alters cortical thickness in adulthood. However, these data are difficult to interpret as it is unknown whether alcohol exposure, an unknown factor, or a pre-existing cortical difference led to heavy binge drinking. Thus, controlled animal studies are needed to directly assess the impact of adolescent binge drinking on cortical thickness.

Animal neuroimaging studies provide a useful tool to directly assess the effect of alcohol on the maturing adolescent cerebral cortex since they allow for the systematic control of extraneous variables. Animal models of adolescent binge drinking reveal ethanol-induced alterations of brain structural volumes that mimic those found in human alcoholics (Coleman et al., 2011; Ehlers et al., 2013; Vetreno et al., 2015). Utilizing diffusion tensor imaging, we previously discovered that adolescent binge ethanol treatment altered adult neocortex structural integrity as evidenced by reductions in both axial and radial diffusivity, which provide measures of the magnitude of water diffusion parallel and perpendicular to axons, respectively (Vetreno et al., 2015). In this study, MRI was used to test the hypothesis that aging and adolescent intermittent ethanol (AIE) treatment of male Wistar rats leads to long-term alterations in cortical thickness. These studies provide novel insight into adult cortical development as well as the impact of adolescent binge drinking on the adult cerebral cortex, which provide validation of the rat cortex as a model to assess the effects of alcohol on the brain.

Materials and Methods

Animals

Young time-mated pregnant female Wistar rats (embryonic day 17; Harlan Sprague-Dawley, Indianapolis, IN) were acclimated to our animal facility prior to birthing at the University of North Carolina at Chapel Hill. On postnatal day (P)1 (24 hr after birth), litters were culled to 10 pups and housed with their dams in standard clear plastic tubs with shavings until group housing with same-sex littermates at the time of weaning on P21. All animals were housed in a temperature- (20°C) and humidity-controlled vivarium on a 12 hr/12 hr light/dark cycle (light onset at 0700 hr), and provided *ad libitum* access to food and water. Experimental procedures were approved by the Institutional Animal Care and Use Committee (IACUC) of the University of North Carolina at Chapel Hill, and conducted in accordance with National Institutes of Health (NIH) regulations for the care and use of animals in research.

Adolescent Intermittent Ethanol (AIE) Treatment Paradigm

On P21, male Wistar rats (N = 20) were randomly assigned to either (i) AIE (n = 10) or (ii) water control (CON; n = 10) groups. Beginning in early adolescence, AIE animals received a single daily intragastric (i.g.) administration of ethanol (5.0 g/kg, 20% ethanol w/v) on a two-day on/two-day off schedule and CON subjects received comparable volumes of water on the same schedule from P25 to P55. Tail blood was collected to assess blood ethanol content (BEC) one hr after ethanol administration as we previously found that BECs in the adolescent rat peak at approximately 60 min following i.g. ethanol administration (Crews et

al., 2006). Further, BECs were assessed at the midpoint of AIE treatment on P38 and again at the conclusion of AIE treatment on P54, and were quantitated using a GM7 Analyzer (Analox, London, UK). On P38 and P54, mean BECs (±S.E.M.) were 166 ± 11 mg/dL and 225 ± 14 mg/dL, respectively. At the conclusion of treatment, subjects were left undisturbed in their home cages, except for weighing, for 25 days until sacrifice on P80. For the duration of AIE exposure, subjects evidenced dramatic increases in body weight that did not differ as a function of treatment (all p±s > 0.05 [P25: CON = 79 ± 2 g, AIE = 79 ± 2 g; P37: CON = 180 ± 3 g, AIE = 175 ± 3 g; P53: CON = 313 ± 4 g, AIE = 303 ± 4 g; P80: CON = 455 ± 7 g, AIE = 449 ± 8 g]). In the aging experiment, a separate group of male Wistar rats (N = 12) received CON water treatment from P25 to P55, and were sacrificed on either P80 (n = 8) or P220 (n = 8) (see Fig. 1). Subjects in the aging cortical thickness study served as controls for comparison to AIE-treated animals in a previously published diffusion tensor imaging study (Vetreno et al., 2015).

Tissue Perfusion for Neuroimaging Studies

On P80 and P220, subjects were anesthetized with a euthanization dose of sodium pentobarbital (100 mg/kg, i.p.). Animals were transcardially perfused on a heating pad with a 1:10 solution of ProHance® (Bracco Diagnositics, Princeton, NJ) in 0.9% saline at 37°C at a flow rate of 30 mL/min followed by 1:10 solution of ProHance® in 10% formalin (pH 7.4) at room temperature (Vetreno et al., 2015). ProHance® is a gadolinium contrast agent that reduces the T1 of the tissues resulting in improved signal to noise and spatial resolution. The skull with brain intact was stored in a specimen container in a 10% formalin solution at 4°C. Twenty-four hr later, the skull with brain intact was transferred to a 1:100 solution of ProHance® in phosphate-buffered saline (PBS, pH 7.4) at 4°C until magnetic resonance image (MRI) processing either at the University of North Carolina at Chapel Hill (aging study) or Duke University (adolescent binge ethanol study).

MRI Image Acquisition – Aging Study

A total of 16 rat skulls with brain intact were sent to the University of North Carolina at Chapel Hill Biomedical Research Imaging Center (BRIC) for MRI in a dedicated 9.4T Bruker small animal scanner. Images were acquired in isotropic voxels (0.16 mm × 0.16 mm × 0.16 mm) using a diffusion-weighted 3D RARE sequence with 12 quasi-uniformly distributed diffusion encoding gradient directions and 3 baseline images. The total scan time was approximately 15 hr per subject.

MRI Image Acquisition – Adolescent Binge Ethanol Study

A total of 20 rat skulls with brain intact were sent to the Duke University Center for *In Vivo* Microscopy for MRI in a 7.0 T Magnex magnet interfaced to an Agilent Direct Drive Console. Specimens where placed in plastic tubes and surrounded with Fomblin, a fluorocarbon used to limit artifacts from susceptibility mismatch between the surface of the brain and air. Data were acquired using a single turn sheet copper solenoid radio frequency coil. Images were acquired using a multi-gradient echo sequence with standard Cartesian encoding. The field of view was 40 mm × 20 mm × 16 mm with an acquisition matrix of 800 × 400 × 320 yielding Nyquist limited isotropic spatial resolution of 50 microns. The acquisition parameters were TR=50 ms, TE1=4.5 ms, and delta TE=9 ms. Four echoes were

acquired at TE=4.5, 13.5, 22.5, and 31.5 ms. All four echoes were averaged to yield a single T2* weighted image for analysis. The flip angle was 60 degrees.

Image Processing

The MRI data was processed using our fully automatic pipeline (Budin et al., 2013). Images were rigidly aligned (translation and rotation) with a pre-existing atlases using mutual information for the aging study (Rumple et al., 2013) and for the AIE study (Calabrese et al., 2013). The rigidly registered T2* images were used for skull stripping the images using an atlas-based tissue classification method (see Oguz et al., 2011). The skull stripped images were deformably co-registered in a group-wise manner to compute an unbiased population average with diffeomorphic non-rigid registration using Advanced Normalization Tools (ANTS; Avants et al., 2009). Each study used pre-existing atlases there were built with Wistar animals, and delineates 30 structures with multi-contrast and oriented in Paxinos-Watson space. The aforementioned atlas segmentation was next registered to the population average and then propagated to the individual subjects for regional volume computation. Rigorous quality control was performed after each step to ensure that automatic processing performance was satisfactory. After registering the population average to the external atlas, the segmentation tissue boundaries of the population average were evaluated to ensure that the segmented regions were accurately described. After propagating the average population labels to individual subjects, an exhaustive quality control of the neocortex segmentation was performed to ensure that the tissue boundaries were well represented in each subject's propagated neocortex.

Neocortex labels extracted from the MR images using the atlas-based algorithm described above were processed to compute cortical thickness measurements. We automatically compute cortical thickness measurements via Laplacian-Partial Differential Equation (PDE) with the use of a correspondence algorithm for statistical analysis. In the Laplacian-PDE based method, the thickness is defined as the length of streamlines crossing cortical layers in perpendicular. Due to the lack of anatomical information, the cortical layers are mathematically derived from the Laplacian vector field. Since the vector field is determined by its boundary condition, it is important to define appropriate boundary conditions in order to create analogous physical layers. Two boundary conditions for the neocortex were defined to ensure accurate cortical thickness measurements: (i) internal cortex layer or rest of the brain, and (ii) external cortex layer or background. While the cortical thickness values computed via the Laplacian-PDE was assigned at each voxel of the segmentation of the image, the measurements for statistical analysis were sampled on the reconstructed surface mesh via correspondence measurements (Cates et al., 2007; Styner et al., 2006). For further details regarding this methodology, refer to Lee et al. (2011).

Tissue Preparation and Immunohistochemistry

At the conclusion of imaging, brain samples were excised from the skull and post-fixed in a 30% sucrose solution for four days at 4°C. Coronal sections were cut (40 μm) on a sliding microtome (MICROM HM450; ThermoScientific, Austin, TX), and sections were sequentially collected into well plates and stored at −20°C in a cryoprotectant solution (30% glycol/30% ethylene glycol in PBS) for later immunohistochemistry.

Free-floating sections (every 6th section) containing the cingulate and retrosplenial cortices were washed in 0.1 M PBS, incubated in 0.3% H_2O_2 to inhibit endogenous peroxidases, and blocked with normal goat serum (MP Biomedicals, Solon, OH). Sections were incubated in mouse polyclonal anti-NEUronal Nuclei (NeuN; Millipore, Temecula, CA) for 24 hr at 4°C. Sections were then washed with PBS, incubated for one hr in biotinylated secondary antibody (goat anti-mouse; Vector Laboratories, Burlingame, CA), and incubated for one hr in avidin-biotin complex solution (Vectastain ABC Kit; Vector Laboratories). The chromagen, nickel-enhanced diaminobenzidine (Sigma-Aldrich, St. Louis, MO), was used to visualize immunoreactivity. Tissue was mounted onto slides, dehydrated with graded alcohol solutions, and coverslipped. Negative control for non-specific binding was conducted on separate sections employing the abovementioned procedures with the exception that the primary antibody was omitted.

Microscopic Quantification and Cortical Thickness Analysis

Immunohistochemical analysis of cortical thickness was focused on sections containing the cingulate and retrosplenial cortices, collectively termed the posterior cingulate cortex, according to the atlas of Paxinos and Watson (1998; Bregma: −0.30 mm to −2.12 mm; see Fig. 2) since MRI revealed bilateral changes in this region in both the aging and AIE experiments. BioQuant Nova Advanced Image Analysis (R&M Biometric, Nashville, TN) was used for image capture on an Olympus BX50 microscope with Sony DXC-390 video camera linked to a computer, and all sections were captured using an Olympus UPlan Fl objective (1.25X/0.30) with a 2X magnifier. Captured images were assessed using ImageJ software (v. 1.48v) available through the NIH and were calibrated to one mm. Vertical cortical thickness through the posterior cingulate cortex was calculated by measuring the distance (mm) from the crest of the genu of the corpus callosum to the outer layer of the dorsal cerebral cortex. Horizontal cortical thickness through the posterior cingulate cortex was calculated by measuring the distance (mm) from the crest of the genu of the corpus callosum to the edge of the medial cerebral cortex. Left and right hemisphere measures were averaged and reported as the cortical thickness. A Pearson's r correlation of cortical thickness measures using immunohistochemistry and MRI in P80 CON subjects revealed that they are comparable methods to measure cortical thickness ($r = 0.81$, $p < 0.01$, $N = 10$; see Fig. 3).

Statistical Analysis

The Statistical Package for the Social Sciences (SPSS; Chicago, IL) was used for all statistical analyses. One-way ANOVAs were used to assess BECs, overall immunohistochemical cortical thickness measures, and brain regional volumes (aging and AIE experiments). The effect of aging and AIE on body weight and cortical thickness across Bregma was assessed using separate repeated measures ANOVAs. Since performing multiple comparisons can increase the incidence of Type I Errors, the Benjamini-Hochberg procedure (B-H Critical) for controlling false positives was calculated (Thissen et al., 2002) for the brain regional volume data. The MRI cortical thickness data was analyzed by computing the mean cortical thickness measurement in each sampled location in the 3D cortex (see Fig. 3). Localized cortical thickness differences were identified by the mean difference. In Fig. 4b and 5b, the mean difference ($\mu_{group1} - \mu_{group2}$) was computed at each

corresponding point in the aging and AIE experiments, respectively. Follow-up Student t-tests for each sampled location were performed to investigate the statistical significance of the initial findings. Although the aging experiment began with 8 subjects per group, several subjects were lost due to technical issues during the MRI scanning procedure. Consequently, there were a total of 5 subjects in the P80 age group and 7 subjects in the P220 age group. Pearson's r correlations were used to assess the association between cortical thickness measures derived from immunohistochemistry and MRI methods. All values are reported as mean ± SEM, and significance was defined at a level of $p \leq 0.05$.

Results

Magnetic resonance imaging (MRI) reveals continued cortical thickness changes during adult rat maturation

Rats continue to grow throughout adulthood (see Fig. 1) and this increase in body weight is paralleled by increases in rat brain regional volumes (Brown et al., 2012; Calabrese et al., 2013; Lebel et al., 2011; Oguz et al., 2013; Sowell et al., 2004b), but the methods for assessing changes in rat brain cortical thickness have only recently been developed (Lee et al., 2011). Comparisons of P80 to P220 brain regional volumes find that the neocortex and corpus callosum undergo significant increases in volume (see Table 1).

To determine if cortical thickness changes in adulthood, we compared MRI measures of cortical thickness in young adult (P80) and more mature adult male Wistar rats (P220). Using a $p = 0.05$ corrected significance level, we found that cortical thickness changed across age from P80 to P220 (see Fig. 4A) with some cortical areas thinning (i.e., P80 > P220) and some cortical regions showing increased thickness (i.e., P220 > P80; see Fig. 4B). Significantly thicker cingulate and retrosplenial cortices as well as areas of the temporal and parietal lobes were observed in P80 rats compared to P220 rats, indicative of cortical thinning in these regions during maturation. In contrast, the prefrontal cortex showed increased cortical thickness in P220 rats than P80 rats. Together, these data suggest that cortical maturation continues past adolescence and into adulthood in the rat.

We focused our follow-up measures in the posterior cingulate cortex and used histology to confirm and extend the MRI findings. Histological evaluation of cortical thickness in the vertical posterior cingulate cortex revealed a 5% (± 1%) reduction in the adult P220 animals, relative to the young adult P80 animals (one-way ANOVA: $F_{(1,16)} = 7.4$, $p < 0.05$; see Fig. 5A). Similarly, analysis of cortical thickness across the horizontal posterior cingulate cortex revealed a 9% (± 1%) reduction in the adult P220 animals, relative to the young adult P80 animals (one-way ANOVA: $F_{(1,16)} = 28.6$, $p < 0.001$; see Fig. 5B). Thus, these data reveal continued age-associated maturational thinning of the posterior cingulate cortex in rats from young adulthood (P80) into mature adulthood (P220).

Structural analysis reveals that AIE treatment alters adult brain regional volumes

In our animal paradigm, human adolescent binge drinking is modeled using an intermittent two-day on/two-day off administration schedule consistent with known heavy patterns of weekend drinking, but not daily drinking associated with alcohol dependence. Adolescent

rats received binge ethanol exposure from P25 to P55, which roughly equates to the early teen to late human adolescent years (i.e., approximately 13 to 25 years of age). To determine the effect of AIE on young adult brain morphology, we used MRI to assess brain regional volumes (mm^3) in structures predicted to change in young adult P80 AIE-treated rats. We found that the total volume of the neocortex, striatum, and amygdala were not changed by AIE treatment in P80 animals 25 days after the last ethanol exposure (see Table 2). However, both corpus callosal and cerebellar volumes were reduced by 4% (± 1%) in the AIE-treated animals, relative to CONs. Furthermore, hippocampal volumes were reduced by 11% (± 2%) in the young adult AIE-treated animals, relative to CONs. In contrast, volumes of the hypothalamus were increased by 6% (± 2%) in the AIE-treated animals, relative to CONs. Taken together, these data reveal that AIE treatment leads to alterations in specific brain regional volumes.

Adolescent binge ethanol treatment alters cortical thickness in the young adult brain

Since we previously found that AIE led to long-term alterations in brain regional volumes and altered neocortical structural integrity (Vetreno et al., 2015), we next sought to determine whether AIE treatment affects cortical refinement in young adulthood. Magnetic resonance imaging was used to assess cortical thickness in CON- and AIE-treated animals that were sacrificed on P80. Using a $p = 0.05$ corrected significance level, we found that AIE treatment altered cortical thickness, relative to age-matched CONs (see Fig. 6A). As depicted in Fig. 6B, we found that AIE treatment led to a small but significant bilateral thinning of the prefrontal cortex. In contrast, AIE treatment was associated with an overall increase in cortical thickness throughout the rest of the cortex, particularly within the cingulate and retrosplenial cortices (i.e., posterior cingulate cortex), relative to CONs. Thus, these data reveal that adolescent binge ethanol exposure alters cortical thickness in young adult rats.

Since the MRI data revealed a significant bilateral increase in cortical thickness of the posterior cingulate cortex following AIE treatment, we used histology to verify the AIE-induced increase in cortical thickness. Histological evaluation of vertical thickness across the posterior cingulate cortex revealed a significant 5% (± 1%) increase in the AIE-treated animals, relative to the CONs (one-way ANOVA: $F_{(1,17)} = 5.2$, $p < 0.05$; see Fig. 7A). Histological evaluation of horizontal cortical thickness of the posterior cingulate cortex did not reveal an effect of AIE treatment (data not shown). To further investigate the AIE-induced changes in the posterior cingulate cortex, we used MRI to assess cortical thickness across the exact regions studied histologically. We found that cortical thickness of the posterior cingulate cortex was significantly increased by 6% (± 1%) in the AIE-treated animals, relative to CONs (main effect of Treatment: $F_{(1,18)} = 6.8$, $p < 0.05$; see Fig. 7B). The AIE-induced increase in cortical thickness across this region is very similar for MRI and histological measures. Indeed, a Pearson's r correlation revealed that histological cortical thickness measures across the posterior cingulate cortex were positively correlated with cortical thickness values obtained from MRI (see Fig. 7C). Together, these data reveal that both histology and MRI provide comparable measures of cortical thickness, and that AIE treatment leads to alterations in cortical thickness that persist into adulthood.

Discussion

To our knowledge, this is the first experiment to use MRI to assess changes in cortical thickness during maturation of the adult rat brain and to determine the long-term effect of adolescent binge ethanol exposure on cortical thickness in the young adult rat brain. We found that volumes of the neocortex and corpus callosum, adjacent gray and white matter structures respectively, are larger in P220 adult rats compared to young adult rats (P80). Assessment of cortical thickness found cortical thinning in both the parietal lobe and posterior frontal lobe of P220 adult animals relative to young adult P80 rats. Interestingly, we found evidence of cortical expansion in the prefrontal cortex of P220 animals relative to the young adult P80 rats. Histological assessment of cortical thickness in the posterior cingulate cortex (i.e., cingulate and retrosplenial cortices) revealed similar age-associated cortical thinning in the P220 adults compared to P80 young adults. We also found that AIE treatment led to long-term alterations in the volume of the corpus callosum, cerebellum, hypothalamus, and hippocampus in the young adult brain. Adolescent intermittent ethanol treatment resulted in a small but significant bilateral thinning of the prefrontal cortex, relative to age-matched controls that was accompanied by a bilateral increase in cortical thickness of the posterior cingulate cortex. Follow-up histological and MRI analysis verified the AIE-induced increase in cortical thickness across this region. Taken together, these data suggest that the cerebral cortex continues to undergo refinement into adulthood and that AIE treatment alters adult cortical thickness that might contribute to the behavioral dysfunction observed in adulthood.

Over the past decade, neuroimaging technology has allowed for non-invasive elucidation of the neuroarchitectural changes that occur in the human brain. Human studies have found brain regional cortical thickness changes throughout life (Sowell et al., 2004b) with some studies suggesting that brain morphology during development is tightly controlled and reflects maturation (Brown et al., 2012). During maturation, both cortical thickness and volume measures show an inverted U-shaped trajectory from early childhood through adolescence that support the transition of the immature human brain to the more efficient adult brain (Amlien et al., 2014; Raznahan et al., 2011; Spear, 2009). Adolescent cortical thinning occurs in a caudal to rostral trajectory (Gogtay et al., 2004) and the trajectory of cortical thickness changes, rather than absolute cortical thickness, appear to be most closely related to the development of intelligence (Schnack et al., 2014; Shaw et al., 2006). Indeed, higher levels of intelligence are associated with more rapid cortical thinning in childhood and adolescence while the pattern of cortical thinning appears to reverse at approximately age 30 such that cortical expansion in adulthood is associated with greater intelligence (Schnack et al., 2014). These human aging data suggest that cortical refinement is never complete, but rather continues through adulthood. In the present study, overall cortical volume did not change as a function of age similar to previous findings (Sullivan et al., 2006), but we did observe significant cortical expansion in the anterior prefrontal cortex of P220 rats, relative to young adult P80 rats, which corresponds to Brodmann Area 10 in the human cortex (Krieg, 1946). In contrast, cortical thinning was observed in the cingulate and retrosplenial cortices (i.e., Brodmann Area 23 and 29b, respectively) as well as the temporal and parietal lobes. Similarly, Brans and colleagues (2010) observed cortical expansion in the

adult human prefrontal cortex, which was associated with higher intelligence, and cortical thinning in both the temporal and parietal cortices. Thus, our findings reveal age-related changes in rat cortical thickness, which appear to model cortical maturation in humans, and might contribute to continued development of cortical function in adulthood.

Neuroimaging studies reveal considerable evidence of regional volume deficits in the adult human alcoholic brain (see e.g., Pfefferbaum et al., 1996). In adolescent binge drinking individuals, similar morphological changes have been observed in the brain (De Bellis et al., 2000; Lisdahl et al., 2013). However, due to the inherent variability associated with human studies, there is considerable variation in adolescent findings that are ascribable, in part, to differences in brain maturation across individuals. Indeed, Lisdahl and colleagues (2013) found that heavy alcohol use during adolescence reduced cerebellum volumes while others report that cerebellar volumes are unaffected (De Bellis et al., 2005). In our AIE paradigm, which models human youthful and adolescent binge drinking but not alcohol dependence associated with alcholism, we found brain regional volumetric reductions of the corpus callosum, hippocampus, and cerebellum of young adult (P80) rats. Ehlers and colleagues (2013) found similar changes in hippocampal volumes of young adult rats following adolescent binge ethanol exposure. Magnetic resonance imaging studies of adolescent binge drinkers reveal altered structural volumes in several brain regions, including the hippocampus and cerebellum (for review, see Welch et al., 2013). We also report here that AIE treatment resulted in reduced cortical thickness in the young adult prefrontal cortex, which corresponds to Brodmann Area 24 (i.e., anterior cingulate cortex; Krieg, 1946). In contrast, AIE treatment led to a bilateral increase in cortical thickness in the posterior cingulate cortex and retrosplenial cortex that correspond to Brodmann Area 23 and 29b. Follow-up histological and MRI analysis verified the AIE-induced increase in cortical thickness across the posterior cingulate cortex. Similarly, in male human adolescents binge drinking in human male adolescents was found to reduce cortical thickness in both the prefrontal and cingulate cortices (Squeglia et al., 2012). The observed increase in cortical thickness in the AIE-treated animals could be related to an ethanol-induced blunting of the maturational processes in the cortex since cortical thinning in humans is associated with increased intelligence (Schnack et al., 2014; Shaw et al., 2006). Thus, AIE-induced alterations would be expected to affect cortical function.

In both human and rodent studies, adolescent binge drinking is associated with deficits in executive functioning. Our laboratory previously found that AIE treatment is associated with persistent reversal learning deficits (Vetreno and Crews, 2012) that might be due to altered cortical functioning. Indeed, functional MRI find that both the orbitofrontal cortex within the prefrontal cortex and anterior cingulate cortex are involved in human reversal learning (Kringelbach and Rolls, 2003), and AIE-induced alterations in maturations of these regions might contribute to the observed reversal learning deficits (Vetreno and Crews, 2012). Furthermore, adolescent binge drinking is associated with an increased risk of developing an alcohol use disorder later in life (DeWit et al., 2000) as well as diminished impulse inhibition (White et al., 2011), reduced attentional functioning (Koskinen et al., 2011), deficits in visuospatial ability (Tapert et al., 2002), and impaired executive functioning (White et al., 2011) that are likely due, in part, to a disruption in normal development of the adolescent prefrontal and cingulate cortices (for a review, see Goldstein and Volkow, 2011).

Although our AIE treatment is not a model of human alcoholism, our findings of changes in brain regional volumes following AIE are consistent with those found in human alcoholics. A younger age of drinking onset is associated with increased risk of lifetime alcohol dependence (DeWit et al., 2000). It is possible that adolescent drinking induces changes in brain maturation that increase risk of alcohol dependence and persist throughout life. Regardless, we report here changes in cortical thickness in young adults that persist long after alcohol exposure.

In summary, cortical thickness changes continue to occur into adulthood. Further, adolescent binge ethanol treatment altered cortical thickness in the young adult, particularly within the frontal, parietal, and temporal lobes. These changes are consistent with underage binge drinking inducing long lasting morphological changes in the developing CNS that may contribute to the persistent neurocognitive deficits associated with adolescent binge drinking.

Acknowledgments

This work was supported in part by the National Institutes of Health, National Institute on Alcoholism and Alcohol Abuse (AA019767, AA11605, AA007573, and AA021040), the Neurobiology of Adolescent Drinking in Adulthood (NADIA [AA020023, AA020024, and AA020022]), National Institute of Biomedical Imaging and Bioengineering Biomedical Technology Resource Center (P41 EB015897; PI: G. Allan Johnson), NIH Shared Instrument Grant (1S10OD010683), and the Bowles Center for Alcohol Studies. The authors thank Dr. Gary Cofer at the Duke Center for In Vivo Microscopy for is assistance in MRI acquisition, Ashley Rumple for data processing and manuscript editing, and Diana Lotito for help with preparation of the manuscript.

References

Amlien IK, Fjell AM, Tamnes CK, Grydeland H, Krogsrud SK, Chaplin TA, Rosa MG, Walhovd KB. Organizing Principles of Human Cortical Development-Thickness and Area from 4 to 30 Years: Insights from Comparative Primate Neuroanatomy. Cereb Cortex. 2014

Avants, BB., Tustison, NJ., Song, G., Gee, JC. Transactions on Medical Imagins Penn Image Computing and Science Laboratory. 2009. ANTS: Open-source tools for normalization and neuroanatomy.

Brans RG, Kahn RS, Schnack HG, van Baal GC, Posthuma D, van Haren NE, Lepage C, Lerch JP, Collins DL, Evans AC, Boomsma DI, Hulshoff Pol HE. Brain plasticity and intellectual ability are influenced by shared genes. J Neurosci. 2010; 30:5519–5524. [PubMed: 20410105]

Brown TT, Kuperman JM, Chung Y, Erhart M, McCabe C, Hagler DJ Jr, Venkatraman VK, Akshoomoff N, Amaral DG, Bloss CS, Casey BJ, Chang L, Ernst TM, Frazier JA, Gruen JR, Kaufmann WE, Kenet T, Kennedy DN, Murray SS, Sowell ER, Jernigan TL, Dale AM. Neuroanatomical assessment of biological maturity. Curr Biol. 2012; 22:1693–1698. [PubMed: 22902750]

Budin F, Hoogstoel M, Reynolds P, Grauer M, O'Leary-Moore SK, Oguz I. Fully automated rodent brain MR image processing pipeline on a Midas server: from acquired images to region-based statistics. Front Neuroinform. 2013; 7:15. [PubMed: 23964234]

Calabrese E, Badea A, Watson C, Johnson GA. A quantitative magnetic resonance histology atlas of postnatal rat brain development with regional estimates of growth and variability. Neuroimage. 2013; 71:196–206. [PubMed: 23353030]

Cates J, Fletcher PT, Styner M, Shenton M, Whitaker R. Shape modeling and analysis with entropy-based particle systems. Inf Process Med Imaging. 2007; 20:333–345. [PubMed: 17633711]

Coleman LG Jr, He J, Lee J, Styner M, Crews FT. Adolescent binge drinking alters adult brain neurotransmitter gene expression, behavior, brain regional volumes, and neurochemistry in mice. Alcoholism, clinical and experimental research. 2011; 35:671–688.

Crews F, He J, Hodge C. Adolescent cortical development: a critical period of vulnerability for addiction. Pharmacology, biochemistry, and behavior. 2007; 86:189–199.

Crews FT, Mdzinarishvili A, Kim D, He J, Nixon K. Neurogenesis in adolescent brain is potently inhibited by ethanol. Neuroscience. 2006; 137:437–445. [PubMed: 16289890]

De Bellis MD, Clark DB, Beers SR, Soloff PH, Boring AM, Hall J, Kersh A, Keshavan MS. Hippocampal volume in adolescent-onset alcohol use disorders. The American journal of psychiatry. 2000; 157:737–744. [PubMed: 10784466]

De Bellis MD, Narasimhan A, Thatcher DL, Keshavan MS, Soloff P, Clark DB. Prefrontal cortex, thalamus, and cerebellar volumes in adolescents and young adults with adolescent-onset alcohol use disorders and comorbid mental disorders. Alcoholism, clinical and experimental research. 2005; 29:1590–1600.

DeWit DJ, Adlaf EM, Offord DR, Ogborne AC. Age at first alcohol use: a risk factor for the development of alcohol disorders. The American journal of psychiatry. 2000; 157:745–750. [PubMed: 10784467]

Ehlers CL, Oguz I, Budin F, Wills DN, Crews FT. Peri-adolescent ethanol vapor exposure produces reductions in hippocampal volume that are correlated with deficits in prepulse inhibition of the startle. Alcoholism, clinical and experimental research. 2013; 37:1466–1475.

Giedd JN. Structural magnetic resonance imaging of the adolescent brain. Annals of the New York Academy of Sciences. 2004; 1021:77–85. [PubMed: 15251877]

Giedd JN, Blumenthal J, Jeffries NO, Castellanos FX, Liu H, Zijdenbos A, Paus T, Evans AC, Rapoport JL. Brain development during childhood and adolescence: a longitudinal MRI study. Nature neuroscience. 1999; 2:861–863. [PubMed: 10491603]

Gogtay N, Giedd JN, Lusk L, Hayashi KM, Greenstein D, Vaituzis AC, Nugent TF 3rd, Herman DH, Clasen LS, Toga AW, Rapoport JL, Thompson PM. Dynamic mapping of human cortical development during childhood through early adulthood. Proc Natl Acad Sci U S A. 2004; 101:8174–8179. [PubMed: 15148381]

Goldstein RZ, Volkow ND. Dysfunction of the prefrontal cortex in addiction: neuroimaging findings and clinical implications. Nature reviews Neuroscience. 2011; 12:652–669. [PubMed: 22011681]

Johnston, LD., O'Malley, PM., Bachman, JG., Schulenberg, JE. Monitoring the Future National Results on drug use: 2012 Overview, Key Findings on Adolescent Drug Use. Institute for Social Research, The University of Michigan; Ann Arbor: 2013.

Koskinen SM, Ahveninen J, Kujala T, Kaprio J, O'Donnell BF, Osipova D, Viken RJ, Naatanen R, Rose RJ. A longitudinal twin study of effects of adolescent alcohol abuse on the neurophysiology of attention and orienting. Alcoholism, clinical and experimental research. 2011; 35:1339–1350.

Krieg WJ. Connections of the cerebral cortex; the albino rat; topography of the cortical areas. J Comp Neurol. 1946; 84:221–275. [PubMed: 20982805]

Kringelbach ML, Rolls ET. Neural correlates of rapid reversal learning in a simple model of human social interaction. Neuroimage. 2003; 20:1371–1383. [PubMed: 14568506]

Lebel C, Roussotte F, Sowell ER. Imaging the impact of prenatal alcohol exposure on the structure of the developing human brain. Neuropsychol Rev. 2011; 21:102–118. [PubMed: 21369875]

Lee J, Ehlers C, Crews F, Niethammer M, Budin F, Paniagua B, Sulik K, Johns J, Styner M, Oguz I. Automatic cortical thickness analysis on rodent brain. Proceedings - Society of Photo-Optical Instrumentation Engineers. 2011; 7962:7962481–79624811.

Lisdahl KM, Thayer R, Squeglia LM, McQueeny TM, Tapert SF. Recent binge drinking predicts smaller cerebellar volumes in adolescents. Psychiatry research. 2013; 211:17–23. [PubMed: 23154095]

Oguz I, Lee J, Budin F, Rumple A, McMurray M, Ehlers C, Crews F, Johns J, Styner M. Automatic Skull-stripping of Rat MRI/DTI Scans and Atlas Building. Proceedings - Society of Photo-Optical Instrumentation Engineers. 2011; 7962:7962251–7962257.

Oguz I, Yaxley R, Budin F, Hoogstoel M, Lee J, Maltbie E, Liu W, Crews FT. Comparison of magnetic resonance imaging in live vs. post mortem rat brains. PloS one. 2013; 8:e71027. [PubMed: 23967148]

Paxinos, G., Watson, C. The rat brain in stereotaxic coordinates. Academic Press; San Diego, CA: 1998.

Pfefferbaum A, Lim KO, Desmond JE, Sullivan EV. Thinning of the corpus callosum in older alcoholic men: a magnetic resonance imaging study. Alcoholism, clinical and experimental research. 1996; 20:752–757.

Raznahan A, Shaw P, Lalonde F, Stockman M, Wallace GL, Greenstein D, Clasen L, Gogtay N, Giedd JN. How does your cortex grow? J Neurosci. 2011; 31:7174–7177. [PubMed: 21562281]

Schnack HG, van Haren NE, Brouwer RM, Evans A, Durston S, Boomsma DI, Kahn RS, Hulshoff Pol HE. Changes in Thickness and Surface Area of the Human Cortex and Their Relationship with Intelligence. Cereb Cortex. 2014

Shaw P, Greenstein D, Lerch J, Clasen L, Lenroot R, Gogtay N, Evans A, Rapoport J, Giedd J. Intellectual ability and cortical development in children and adolescents. Nature. 2006; 440:676–679. [PubMed: 16572172]

Sowell ER, Thompson PM, Leonard CM, Welcome SE, Kan E, Toga AW. Longitudinal mapping of cortical thickness and brain growth in normal children. J Neurosci. 2004a; 24:8223–8231. [PubMed: 15385605]

Sowell ER, Thompson PM, Toga AW. Mapping changes in the human cortex throughout the span of life. Neuroscientist. 2004b; 10:372–392. [PubMed: 15271264]

Spear, LP. The behavioral neuroscience of adolescence. 1. W. W. Norton & Co Inc; New York: 2009.

Squeglia LM, Sorg SF, Schweinsburg AD, Wetherill RR, Pulido C, Tapert SF. Binge drinking differentially affects adolescent male and female brain morphometry. Psychopharmacology. 2012; 220:529–539. [PubMed: 21952669]

Styner M, Oguz I, Xu S, Brechbuhler C, Pantazis D, Levitt JJ, Shenton ME, Gerig G. Framework for the Statistical Shape Analysis of Brain Structures using SPHARM-PDM. Insight J. 2006:242–250. [PubMed: 21941375]

Sullivan EV, Adalsteinsson E, Sood R, Mayer D, Bell R, McBride W, Li TK, Pfefferbaum A. Longitudinal brain magnetic resonance imaging study of the alcohol-preferring rat. Part I: adult brain growth. Alcohol Clin Exp Res. 2006; 30:1234–1247. [PubMed: 16792572]

Tapert SF, Baratta MV, Abrantes AM, Brown SA. Attention dysfunction predicts substance involvement in community youths. Journal of the American Academy of Child and Adolescent Psychiatry. 2002; 41:680–686. [PubMed: 12049442]

Thissen D, Steinberg L, Kuang D. Quick and easy implementation of the Benjamini-Hochberg procedure for controlling the false positive rate in multiple comparisons. Journal of Educational and Behavioral Statistics. 2002; 27:77–83.

Toga AW, Thompson PM, Sowell ER. Mapping brain maturation. Trends Neurosci. 2006; 29:148–159. [PubMed: 16472876]

Vetreno RP, Crews FT. Adolescent binge drinking increases expression of the danger signal receptor agonist HMGB1 and Toll-like receptors in the adult prefrontal cortex. Neuroscience. 2012; 226:475–488. [PubMed: 22986167]

Vetreno RP, Yaxley R, Paniagua B, Crews FT. Diffusion tensor imaging reveals adolescent binge ethanol-induced brain structural integrity alterations in adult rats that correlate with behavioral dysfunction. Addict Biol. 2015

Welch KA, Carson A, Lawrie SM. Brain structure in adolescents and young adults with alcohol problems: systematic review of imaging studies. Alcohol and alcoholism. 2013; 48:433–444. [PubMed: 23632805]

White AM, Kraus CL, Swartzwelder H. Many college freshmen drink at levels far beyond the binge threshold. Alcoholism, clinical and experimental research. 2006; 30:1006–1010.

White HR, Marmorstein NR, Crews FT, Bates ME, Mun EY, Loeber R. Associations between heavy drinking and changes in impulsive behavior among adolescent boys. Alcoholism, clinical and experimental research. 2011; 35:295–303.

Windle M, Spear LP, Fuligni AJ, Angold A, Brown JD, Pine D, Smith GT, Giedd J, Dahl RE. Transitions into underage and problem drinking: developmental processes and mechanisms between 10 and 15 years of age. Pediatrics. 2008; 121(Suppl 4):S273–289. [PubMed: 18381494]

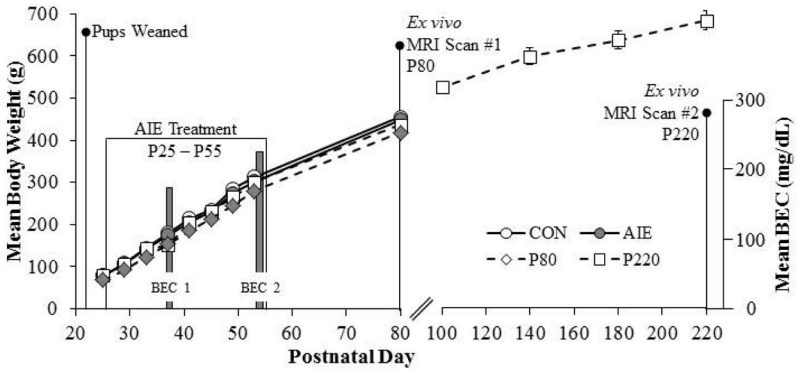

Figure 1. Graphical representation of the adolescent intermittent ethanol (AIE) treatment paradigm

Rats received either ethanol (5.0 g/kg, 20% ethanol w/v, i.g.) or a comparable volume of water from postnatal day (P)25 to P55 on a two-day on/two-day off administration schedule. Blood ethanol concentrations (BECs) were assessed one hr after ethanol exposure on P38 and P54. Subjects were sacrifice on P80 for magnetic resonance imaging (MRI) analysis of cortical thickness. Subjects in the aging experiment were sacrificed either on P80 or P220 for MRI analysis of cortical thickness.

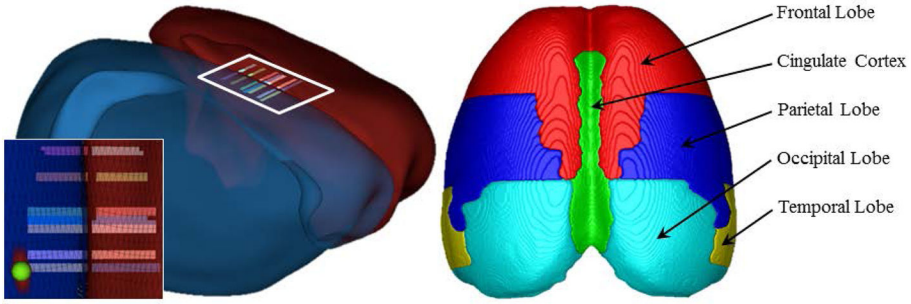

Figure 2. Representative scans depicting parameters for assessment of cortical thickness

(A) Schematic highlighting the cingulate and retrosplenial cortices assessed for cortical thickness using magnetic resonance imaging. Stripped areas in the 3D surface model correspond to areas where cortical thickness was also assessed histologically. (B) Schematic depicting the major lobes of the young adult (postnatal day 80) rat brain.

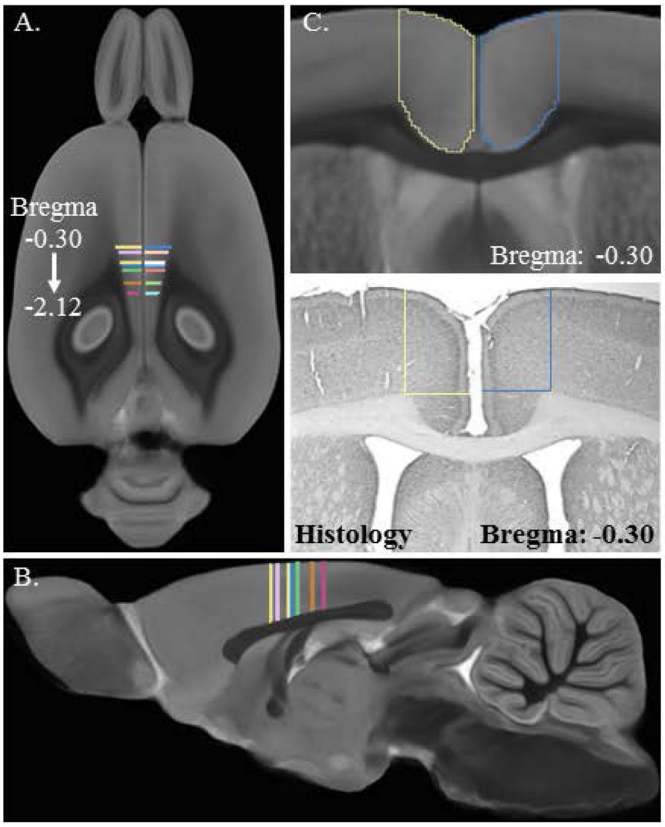

Figure 3. Experimental design of the cortical thickness validation study

(A) Horizontal and (B) sagittal views of the multi-gradient echo (GRE) magnetic resonance imaging (MRI) population average with marked Bregma-matching areas in the cingulate and retrosplenial cortices in which cortical thickness was measured in both MRI and histology. (C) Schematic showing a close-up of the same coronal location for MRI and histology where cortical thickness was analyzed.

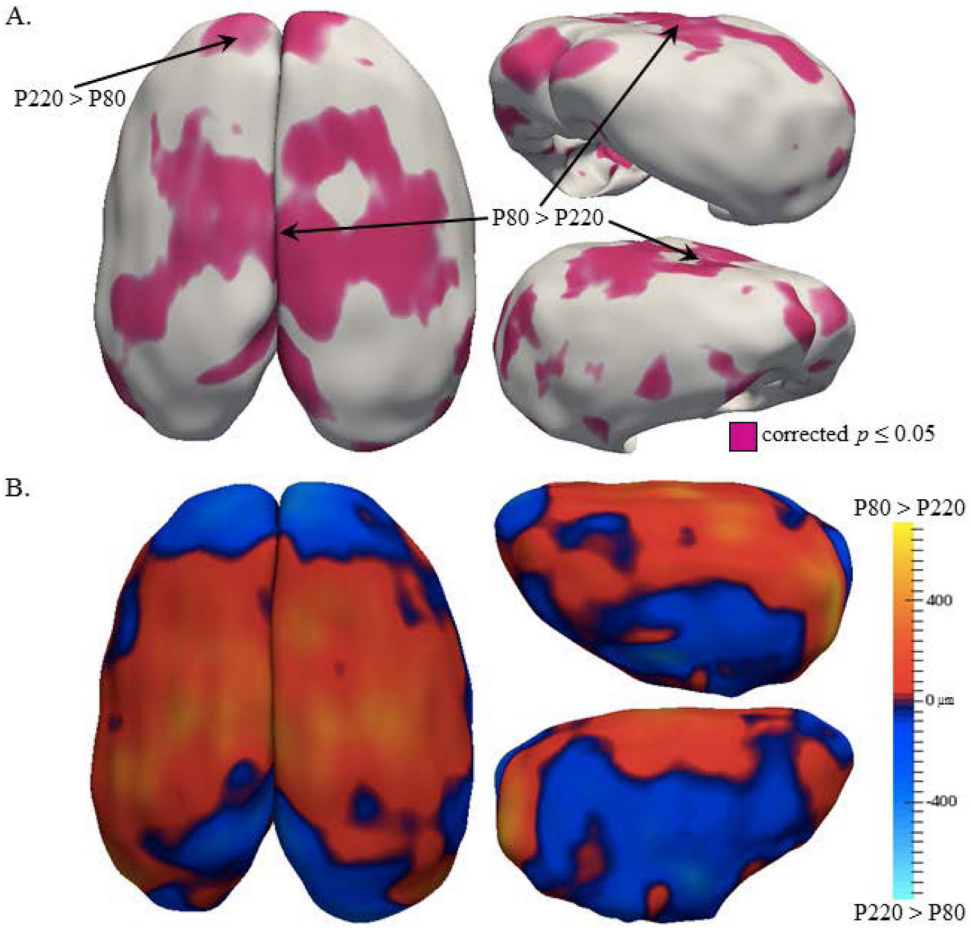

Figure 4. Results of the cortical thickness analysis in the aging study

(A) Significance probabilities of paired Student's t-test are mapped on the 3D cortical surface with purple color for highly significant regions ($p < 0.05$) and gray for low. All p-values are False Discovery Rate corrected with a 10% threshold. (B) The direction of mean thickness differences between the P80 and P220 groups are depicted with red shades indicating regions where the P80 cortex is thicker (cortical thinning), and blue shades indicating regions where the P220 group is thicker (cortical growth). Mean thickness differences are color-mapped on the average cortex 3D surface with 25,002 corresponding points. Measurements range from −800 µm to +800 µm. The frontal and occipital lobes show a pattern of cortical expansion while the rest of the brain shows a generalized pattern of cortical thinning.

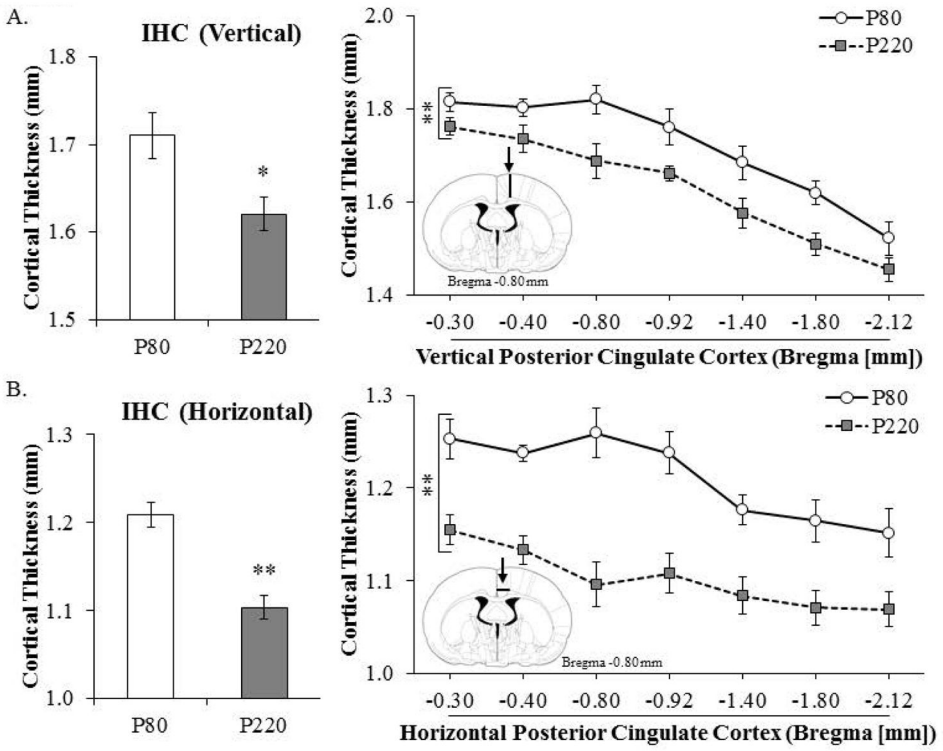

Figure 5. Immunohistochemistry reveals cortical thinning in the aging cortex

(A) Across aging, there was a 5% (± 1%) reduction in the cortical thickness of the vertical posterior cingulate cortex from postnatal day (P)80 to P220. (B) Measures of cortical thickness across the horizontal cingulate cortex show an age-associated 9% (± 1%) reduction from P80 to P220. Presented are mean ± S.E.M. * $p < 0.05$, ** $p < 0.01$.

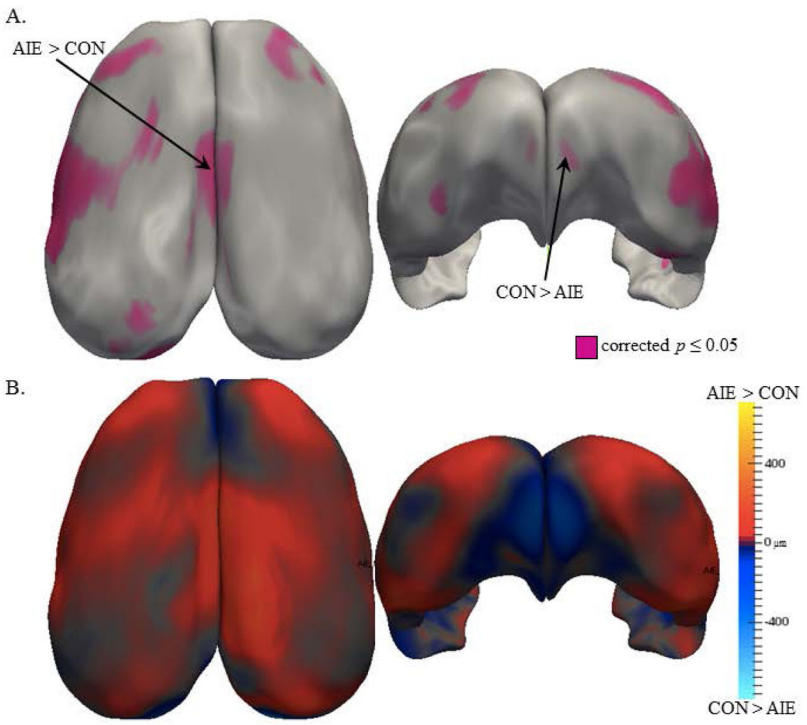

Figure 6. Results of the cortical thickness analysis in the adolescent intermittent ethanol (AIE) study

(A) Significance probabilities of paired Student's t-test are mapped on the surface of the average 3D cortex with purple color for highly significant regions ($p < 0.05$) and gray for low. All p-values are False Discovery Rate corrected with a 10% threshold. (B) The direction of mean thickness differences between the AIE and CON groups are depicted with red shades indicating regions where the AIE cortex is thicker, and blue shades indicating regions where the CON group is thicker. Mean thickness differences are color-mapped on the average cortex 3D surface with 25,002 corresponding points. Measurements range from −800 µm to +800 µm. Adolescent intermittent ethanol treatment caused thinning of the prefrontal cortex, but thickening in the cingulate and retrosplenial cortices.

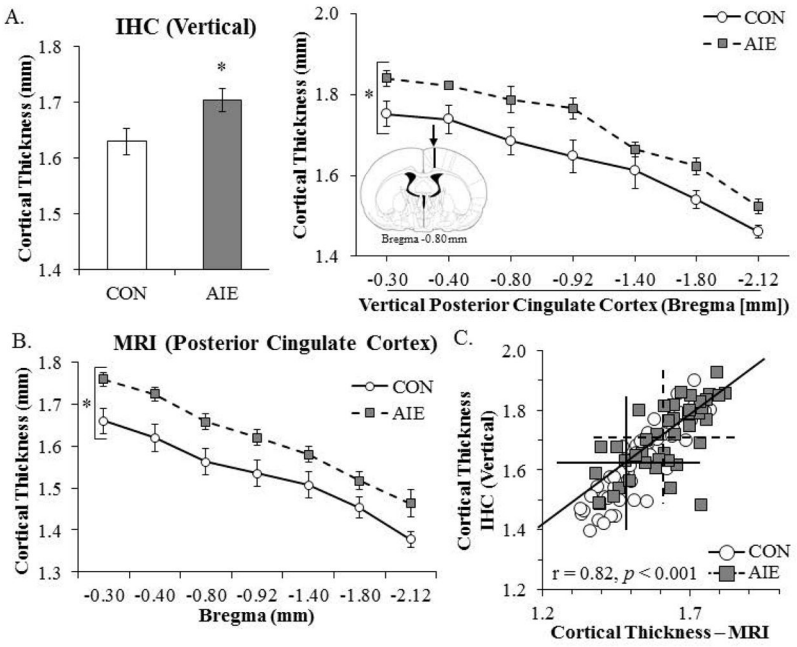

Figure 7. Immunohistochemistry and magnetic resonance imaging (MRI) reveal cortical expansion in the cortex of adolescent intermittent ethanol (AIE)-treated young adult animals

Histology and MRI was used to assess cortical thickness in young adult rats (postnatal day 80) following AIE treatment. (A) Adolescent intermittent ethanol treatment led to a 5% (± 1%) increase in cortical thickness of the vertical posterior cingulate cortex, relative to age-matched controls. (B) Graph showing average MRI-derived cortical thickness measurements from the posterior cingulate cortex. Ethanol-exposed animals show increased cortical thickness. Presented are mean ± S.E.M. * $p < 0.05$. (C) Immunohistological (IHC) assessment of cortical thickness within the vertical posterior cingulate cortex correlates with MRI-derived measurements. The crossed lines indicate the mean values for the CON- (solid) and AIE-treated (dashed) subjects.

Table 1

Magnetic resonance imaging (MRI) analysis of brain regional volumes across aging.

	Regional Volume (mm^3)			
Region	**P80**	**P220**	***p*-value**	**B-H Critical**
Hypothalamus	66.22	65.73	0.467	0.0107
Hippocampus	100.49	102.43	0.383	0.0143
Amygdala	21.06	20.23	0.359	0.0250
Cerebellum	295.18	284.17	0.336	0.0214
Striatum	88.2	82.6	0.245	0.0036
Corpus Callosum	***6.45***	***8.59***	***0.008***	***0.0179***
Neocortex	***624.19***	***715.67***	***0.002***	***0.0071***

The effect of aging on select brain regional volumes using MRI at postnatal day (P)80 and P220. Mean volumes of the individual structures (mm^3) in P80 and P220 groups, the *p*-value (t-test), and Benjamini-Hochberg procedure (B-H Critical) for controlling false positives are shown. An individual t-test is significant if the *p*-value is ***less than*** the B-H Critical value.

Table 2

Magnetic resonance imaging (MRI) analysis of brain regional volumes across treatment.

	Regional Volume (mm^3)			
Region	**CON**	**AIE**	***p*-value**	**B-H Critical**
Neocortex	506.49	508.36	0.343	0.025
Striatum	75.96	76.82	0.293	0.021
Amygdala	39.18	38.43	0.093	0.018
Corpus Callosum	*86.61*	*83.07*	*0.019*	*0.014*
Cerebellum	***266.72***	***255.62***	***0.008***	***0.011***
Hypothalamus	***30.34***	***32.23***	***0.007***	***0.007***
Hippocampus	***103.73***	***92.63***	***0.003***	***0.004***

The effect of adolescent intermittent ethanol (AIE) treatment on select young adult brain regional volumes using MRI at postnatal day 80. Mean volumes of the individual structures (mm^3) in CON and AIE groups, the *p*-value (t-test), and Benjamini-Hochberg procedure (B-H Critical) for controlling false positives are shown. An individual t-test is significant if the *p*-value is ***less than*** the B-H Critical value. Although the corpus callosum volumes differ based on t-test analysis (*italic*), it did not meet the B-H Critical threshold for false positive control.